RSC Advances

Performance comparison of activated carbon and ferric oxide-hydroxide - activated carbon nanocomposite as vanadium (v) ions adsorbents

Journal:	*RSC Advances*
Manuscript ID	RA-ART-07-2015-014493.R1
Article Type:	Paper
Date Submitted by the Author:	30-Aug-2015
Complete List of Authors:	Sharififard, hakimeh; Amirkabir University of Technology, Soleimani, Mansooreh; Amirkabir University of Technology, Chemical Engineering Department

RSC Advances

ARTICLE

Performance comparison of activated carbon and ferric oxide-hydroxide - activated carbon nanocomposite as vanadium (v) ions adsorbents

Received 00th January 20xx,
Accepted 00th January 20xx

DOI: 10.1039/x0xx00000x

www.rsc.org/

Hakimeh Sharififard[a], Mansooreh Soleimani[a,]*

Recently, a great deal of attention has been paid to water treatment using nanoparticles such as ferric nanoparticles. In this work,the ferric oxide-hydroxide -activated carbon nanocomposite (Fe-AC) was synthesized via a simple and low-temperature method and characterized using BET, XRF, FTIR, XRD and SEM techniques. In order to compare the performance of commercial activated carbon (CAC) and Fe-AC for vanadium ions adsorption, the influences of various adsorption parameters such as pH, contact time, initial concentration of vanadium and temperature were investigated. The kinetic data confirmed the validity of the pseudo-second-order kinetic model for CAC and Fe-AC. The sorption isotherms were studied using Langmuir, Freundlich, and Dubinin–Radushkevich (D–R) isotherm models. The equilibrium data was described with significant accuracy by using the Freundlich model. The results showed that CAC had a vanadium ions adsorption capacity of 37.87 mg g^{-1},while Fe-AC was able to adsorb 119.01 mg g^{-1} of vanadium. The determination of different thermodynamic parameters indicated that the vanadium ions adsorption was feasible, spontaneous and that both adsorbents had an exothermic nature.

Introduction

Nowadays, the application of nanotechnology for water and wastewater treatment has become a subject of considerable attention and concern. Nanoparticles are one of the most important structures in nanotechnology. The most important property of nanoparticles is their high reactivity due to their large surface to volume ratio, which can be utilized for different applications in many fields. Among different nanoparticles, ferric nanoparticles have attracted extensive interest due to their superparamagnetic, high reactivity and non-toxic properties. These nanoparticles are used in various fields such as terabit magnetic storage devices, catalysis, sensors, high-sensitivity biomolecular magnetic resonance imaging (MRI) and wastewater treatment. Ferric nanoparticles have been used as an adsorbent for heavy metals removal, precious metals recovery and dye removal. Also, these nanoparticles can be used for modifying the commercial adsorbents [1-12].

Activated carbon has been a preferred adsorbent for many years in major industrial applications especially water and wastewater treatment processes due to its high adsorption capacity, high adsorption rate and good resistance to abrasion [13-17]. However, its ability to adsorb inorganic ions is less than that for organic compounds.

[a] *Department of Chemical Engine*ering, Amirkabir University of *Technology, No. 424, Hafez Ave., P.O* .Box 15875-4413, Tehran, Iran; E-mail: Soleimanim@aut.ac.ir, Tel. & Fax: +98(21) 66405847.

The increased use of activated carbon has made it imperative to improve the adsorption properties of activated carbon for inorganic and organic ions [18-19]. The modification of activated carbon with ferric nanoparticles is a new and good way to provide high adsorption capacity for inorganic and organic ions such as Pb(II), nitrate, cyanide and arsenic (due to providing porous media that is charged with iron ions) [20-23].

Different technologies such as evaporation of ferric salt in the presence of activated carbon, iron precipitation with alkaline solutions and the oxidation/precipitation of iron have been proposed for anchorage of ferric nanoparticles onto activated carbon surfaces [24,25]. However, energy consumption for some of the methods is very high [23]. Anchorage is a simple method for the synthesis of ferric nanoparticles-activated carbon composite which consists of using a solution of ferric salt [18].

Vanadium is a well-known toxic metal and exists in the environment as tetravalent [V(IV)] and pentavalent [V(V)] forms of which the pentavalent form is more toxic than the tetravalent one [26-28]. The Occupational Safety and Health Administration (OSHA) has determined that exposure to vanadium pentoxide dust and vanadium fumes should be limited to 0.5 and 0.1 mg m^{-3}, respectively during an 8 h work day [28]. This metal is widely used in many industries such as glass, steel, textile, ceramic, photography, metallurgy and the plants producing industrial inorganic chemicals and pigments. The discharge of vanadium from these industries into the environment especially steel slags discharge can cause serious environmental

problems. Vanadium has been discharged into the environment from oil refineries and power-plants in the form of vanadium rich oil fuel and coal. Due to the environmental risks, it is necessary to remove vanadium from the industrial effluents such as steel and oil slags. Different technologies such as extraction, membrane technology, and adsorption have been studied to remove vanadium from wastewater [28-30]. Among these technologies, adsorption is more advantageous due to its high separation efficiency, low cost, and easy operation [20]. Based on the published papers, this paper is the first study to suggest the use of a composite of ferric oxide-hydroxide nanoparticles (one kind of ferric nanoparticles) and activated carbon for vanadium ions adsorption. In this work, the ferric oxide-hydroxide - activated carbon (Fe-AC) nanocomposite was synthesized via a low temperature and simple method and characterized using different analyzing techniques.

The main objectives of the present study include the following:

1. To synthesize nanocomposite of Ferric oxide-hydroxide-activated carbon (Fe-AC) via low temperature and simple method as a new adsorbent for vanadium.
2. To compare the adsorption ability of commercial activated carbon (CAC) and Fe-AC.
3. To investigate the influences of various adsorption parameters such as pH, time, initial concentration and temperature.
4. To analyze the kinetic and equilibrium data for understanding the adsorption mechanism.

Materials and methods

Materials

The commercial activated carbon (CAC) used in this study, was Norit ROY 0.8 manufactured by Norit. The size of activated carbon was 300-500 µm (mesh no. 35-50). Ferrous sulfate ($FeSO_4 \cdot 7H_2O$), vanadium pentoxide, sodium hydroxide, sulfuric acid, hydrochloride acid and sodium carbonatewere purchased from Merck company. The solution was prepared using ultrapure deionized water (18.3 MΩ·cm) produced from a Milli-Q water purification system.

Synthesis of Fe-AC

To synthesize Fe-AC, 10 g of the CAC sample was mixed with 200 mL of 0.6 M Fe (SO_4) $7H_2O$ solution inside a sealed glass container. The sample was placed in an agitating incubator (NB-205, N-BIOTECK) at 55 ºC for 24 h. Finally, the mixture was filtered with filter paper (Whatman No. 42) and the Fe-AC sample was rinsed with ultrapure water until all soluble iron and iron particles that were not anchored to the surface of CAC were removed. To ensure this, the iron of washing water was analyzed using an atomic absorption spectrophotometer (AAS) (Varian AA240). The sample was dried in an air oven at 60 C for 24 h and the dried samples of adsorbents (CAC and Fe-AC) were kept in a desiccator [18,19]. After preparing Fe-AC, the iron leaching tests were conducted to investigate the stability of iron nanoparticles on CAC surface. Doing this, 0.05 g of the Fe-AC was agitated (N-BIOTECK, NB-205) with 25 mL of HCl solution at different pH (2, 4, 5, 6) at 25 ºC for 6 h. After filtration of sample, the concentration of iron ions was determined in the solution by AAS. These results indicated that there is no measurable amount of iron in the samples.

Characterization of adsorbents

The adsorbents were characterized by selected physical and chemical properties:

- The pH_{ZPC} (point of zero charge) of CAC and Fe-AC was measured by the following method:0.3 g of adsorbent was added to 50 mL of a 0.1 N NaCl solution, where the initial solution pH was adjusted using aqueous HCl or NaOH solutions. If the initial pH of the solution is equal to the pH_{ZPC} of the adsorbent, no change in the pH will be observed after adding adsorbent to the solution [31].
- The morphologies of CAC and Fe-AC were determined by direct measurement on scanning electron micrographs (SEM, Seron Technology, AIS2100).
- The porous texture and surface area of samples were determined from adsorption−desorption isotherms of N_2 at 77 $^{\circ}K$ using an automatic volumetric system (Quantachrome NOVA 1000). The surface areas were calculated by applying the BET (Brunauer−Emmett−Teller) method. The volume (mL g^{-1}) and width ($^{\circ}A$) of micropore and mesopore were determined by HK (Horvath−Kawazoe) and BJH (Barrett, Joyner, and Halenda) methods respectively[32,33]. The total pore volume of the sample was determined from the amount of nitrogen adsorbed at the highest relative pressure examined. The mean pore width ($^{\circ}A$) was calculated from the $4V_{tot}/S_{BET}$ relation. The pore size distribution of adsorbents was determined by using the density function theory (DFT).
- The surface chemistry of the adsorbents was determined using Fourier transform infrared radiation (Nicolet FT-IR spectrophotometer, NEXUS 670), 4 cm^{-1} resolution, sample/KBr =1/100) within the range of 400–4000 cm^{-1} wave number.
- The XRF analysis was carried out using X-ray fluorescence (XRF, unisantis, XMF-104) in order to determine the amount of iron which anchorage on CAC.
- X-ray diffraction (XRD) spectra of the Fe-AC sample was analyzed using a high-resolution X-ray diffractometer (XRD, Philips X' Pertdiffractometer, Cu Kα rad).

Adsorption experiments

Effect of pH

To determine the effect of the initial pH of the solutions on the vanadium ions adsorption, a series of batch experiments were conducted at different initial pH values ranging from 1 to 9. The other operating conditions were as follows: initial vanadium concentration= 60 mg L^{-1}, adsorbent dosage =1 g L^{-1}, agitation rate =250 rpm, temperature = 25 °C and agitation time =3 h. After this time, the solution was filtered and residual was analyzed for vanadium concentrationusing atomic absorption spectroscopy (AAS) (Varian AA240, wavelength of 318 nm).

The adsorption percentage of vanadium was determined from Eq. (1):

$$\text{Adsorption (\%)} = \frac{(C_0 - Cf)}{C_0} \times 100 \quad (1)$$

In this equation, C_0 and C_f are the initial and final metal ion concentration (mg L^{-1}), respectively.

Kinetics studies

Adsorption kinetic experiments were studied by placing 0.05 g adsorbents (CAC, Fe-AC) in flasks containing 50 mL (60 mg L^{-1}) of metal ion solution at an initial pH of 4.5. The contents of the flasks were agitated by an orbital agitator (FINEPCR-SH30) at 250 rpm for the prescribed periods of time at 25 $^{\circ}C$. After these periods of time

and filtration, the concentration of the solutions was analyzed using AAS (Varian AA240, the wavelength of 318 nm). The amount of vanadium adsorbed by CAC and Fe-AC, q, was determined by the following equation:

$$q = \frac{V}{m}(C_0 - C_f) \quad (2)$$

where V and m are the solution volume (L) and dry weight of adsorbent (g) respectively.

Kinetics models

Since investigation of the controlling mechanisms of the adsorption process such as mass transfer and chemical reaction is important, the pseudo-first-order, pseudo-second-order, Intra-particle diffusion and Boyd equations are applied to model the kinetics of vanadium ions adsorption. These models are presented in Table 1.

Equilibrium experiments

To evaluate the performance of CAC and Fe-AC for vanadium ions adsorption, the equilibrium studies of the vanadium removal with these adsorbents were carried out by placing 0.05 g of each adsorbent in a series of flasks containing 50 mL of vanadium ions solution at different initial concentrations (25-200 mg L^{-1}) and initial pH of 4.5. The flasks were agitated on an orbital agitator incubator (N-BIOTECK, NB-205) at 250 rpm for 24 h at various temperatures (25 ºC, 35 ºC, 45 ºC). After this period, the metal solutions were filtered and the residual concentration of the metal ions was determined by AAS. The amount of vanadium ions adsorbed by these adsorbents, q, was determined by Eq. (2).

Equilibrium isotherms

The three most widely used adsorption isotherms are theLangmuir, Freundlich and Dubinin–Radushkevich (D-R) isotherms. In this work, the experimental data was analyzed based on these three isotherms.

Table 1 Kinetics models*

Kinetic model	Equation
Pseudo-first-order	$\log(q_e - q) = \log q_e - \frac{k_1 t}{2.303}$
Pseudo-second-order	$\frac{t}{q} = \frac{1}{k_2 q_e^2} + \frac{1}{q_e} t$
Intra-particle diffusion	$q_t = k_{id} t^{0.5}$
Boyd model	$Bt = -0.4977 - \ln(1 - F)$
	$B = \frac{\pi^2 D_i}{r^2}$
	$F = q/q_e$

*Description of parameters is presented in Notation table.

The Langmuir adsorption isotherm equation in linear form is given as:

$$\frac{1}{q_e} = \frac{1}{q_{\max} . K_L} . \frac{1}{C_e} + \frac{1}{q_{\max}} \quad (3)$$

where q_{max} is the maximum adsorption capacity of the adsorbent (mg g^{-1}), and K_L is the Langmuir constant related to energy of adsorption (L mg^{-1}).

The linear form of the Freundlich model is:

$$\log q_e = \frac{1}{n} \log C_e + \log K_f \quad (4)$$

In this equation, K_f ($mg^{1-(1/n)}$ $L^{1/n}$ g^{-1}) is the Freundlich constant related to adsorption capacity of the adsorbent and n is the Freundlich–exponent related to adsorption intensity.

The Dubinin–Radushkevich (D-R) isotherm was applied to determine whether the nature of adsorption is physical or chemical. The linear form of the Dubinin-Radushkevich isotherm is:

$$\ln q_e = \ln q_m - \beta \varepsilon^2 \quad (5)$$

where q_m is the theoretical saturation capacity (mol g^{-1}), β is a constant term related to the mean free energy of adsorption per mole of the adsorbate (mol^2 J^{-2}), and ε is the Polanyi potential which is related to the equilibrium concentration as follows:

$$\varepsilon = RT \ln\left(1 + \frac{1}{C_e}\right) \quad (6)$$

where R is the universal gas constant (8.314 J mol^{-1} K^{-1}), C_e is the equilibrium concentration of adsorbate in solution (mol L^{-1}), and T (°K) is the absolute temperature. A plot of $\ln q_e$ versus ε^2 is used to determine the D-R constants q_m and β. The constant β gives an idea about the mean free energy E (kJ mol^{-1}) of adsorption per molecule of the adsorbate when it is transferred to the surface of the solid from infinity in the solution, and can be calculated using the following equation:

$$E = \frac{1}{(2\beta)^{1/2}} \quad (7)$$

This parameter will determine whether the adsorption mechanism has an ion-exchange nature or a physical adsorption nature. If the magnitude of E is between 8 and 16 kJ mol^{-1}, the adsorption process follows an ion-exchange nature (chemical nature), whereas for the values of E < 8 kJ mol^{-1}, the adsorption process has a physical nature [34].

Reuse of adsorbents

In order to investigate the reuse of adsorbent, firstly the adsorption of vanadium using CAC and Fe-AC was investigated by contacting 0.1 g of adsorbent with 100 mL of vanadium solution (60 ppm) at 25 ºC and pH 4.5 for 4 h. At the end of each the adsorption test, the adsorbent was filtered, washed with distilled water to remove the un-adsorbed vanadium ions and dried in an oven at 70 ºC for 3 h. The residual solution was then analyzed for vanadium concentration using AAS. The adsorption percentage of vanadium was determined from Eq. (1). Subsequently, desorption experiment was performed as follow:

0.1 g of the V(V)-loaded adsorbent was agitated (on N-BIOTECK, NB-205) with 50 mL of 0.1 M HCl solution at a speed of 200 rpm at 25 ºC for 4 h. After filtration, the concentration of vanadium ions was determined in the solution by AAS. The percentage of desorption was calculated by dividing the amount of vanadium ions

desorbed by the amount of metal ions adsorbed. The adsorption-desorption cycle was performed four times.

Results and discussion

Characterization of adsorbents

The pH_{ZPC} of CAC and Fe-AC samples were 6.1 and 5.4, respectively. The slight decrease of pH_{ZPC} is attributed to the formation of ferric nanoparticles on the surface of CAC.

To clearly understand the average particle size and morphology of nano scale ferric on the surface of activated carbon, samples were characterized by scanning electron microscopy. Fig. 1 shows the SEM microscopies of the CAC and Fe-AC nanocomposite. It revealed the presence of ferric nanoparticles inside the pores and on the surface of Fe-AC media. The ferric nanoparticles were widely distributed on the CAC surface. The size of these nanoparticles ranged from40 nm to 90 nm.

Nitrogen adsorption-desorption isotherms for the two samples are presented in Fig. 2a. The results show that the adsorption-desorption isotherms of the samples are similar, and it can be concluded that these isotherms belong to the combination of type I and type II in IUPAC classification[35,36]. These types of isotherms can be commonly observed in porous systems with a combination of micro- and mesopores. The small hysteresis loops of the isotherms are the H4 class, which are often associated with narrow slit-like pores with a regular structure[37].

The porosity parameters of the adsorbents have been derived from N_2 adsorption−desorption data and are reported in Table 2. It can be seen that the formation of ferric nanoparticles inside and outside the porous structure of the CAC causes a reduction in BET surface area and pore volume (micro and mesopore).The results show that the percentages of micropores and mesopores were decreased by the formation of nanoparticles on the surface of CAC. Therefore, it can be concluded that the molecules of ferric diffuse into the micro- and mesopore structure of CAC and limit the accessibility of N_2 molecules to micro- and mesopores. As a result, the average pore width of the Fe-AC sample (in the micro and meso ranges) increases more compared to CAC. The pore size distribution of adsorbents evaluated by the density function theory is illustrated in Fig. 2b. This figure confirms that the pores of samples are mainly in the micropores region. Similar to the results presented in Table 2, the DFT approach showed a decrease in the total pore volume for Fe-AC due to the ferric nanoparticles deposition.

The FTIR spectra of CAC and Fe-AC samples are presented in Fig. 3. The bands at 3434 cm^{-1} and 3388 cm^{-1} represent the absorption of water molecules, which cause hydroxyl groups (O-H) to form on the surface of CAC and Fe-AC respectively[38]. The peaks at around 2930 cm^{-1}, 2850 cm^{-1}, and 1630 cm^{-1} for two samples and 1455 cm^{-1} for CAC represent C-H aliphatic stretching, $–O–CH_3$ of the aldehyde group, stretching vibrations of C=O in carbonyl, lactone and carboxyl groups, and stretching of C–O or O–H deformation in carboxylic acids respectively[39].

In the FTIR spectra of Fe-AC, the 1455 cm^{-1} peak is shifted to 1574 cm^{-1}, and this indicates the chemical interaction of ferric with carboxylic acids of CAC. The new peaks are at 409 cm^{-1}, 882-790 cm^{-1}, and 638 cm^{-1} for Fe-AC. These new peaks confirm the formation of Fe-OH, Fe-O, and C-O-Fe bonds[40,41]. The new bands are also observed between 1200.51 cm^{-1} and 1086 cm^{-1}, which could be attributed to the presence of SO_4^{2-} in Fe-AC[18]. The SO_4^{2-}, OHand iron species can create iron oxide-hydr(oxide) types such as FeOOH and $FeOHSO_4$ according to the following sequence:

$$2FeSO_4 + O_2 + H_2O \rightarrow FeOHSO_4 + FeOOH \quad (8)$$

The iron contents of CAC and Fe-AC were <0.2 wt. % and 12.57 wt.% respectively. The structure of the iron nanoparticles on AC surface was verified by XRD patterns shown in Fig.4. This figure shows the nanocrystallite peaks matching well with the standard FeOOH (00-003-0251).

Table 2 Porosity parameters of CAC and Fe-AC samples

Parameters	CAC	Fe-AC
BET Sp Surf. Area (m2 g-1)	1070.000	711.600
Total pore volume (mL g-1)	0.660	0.444
Micropore volume(mL g-1), HK method	0.530	0.335
Mesopore volume (mL g-1), BJH method	0.130	0.110
Volume percentage occupied by micropores	80.000	75.400
Average micropore width(ºA), HK method	15.500	16.400
Average mesopore width(ºA), BJH method	22.500	23.300
Average pore width(ºA), 4Vtot/SBET	24.670	24.950

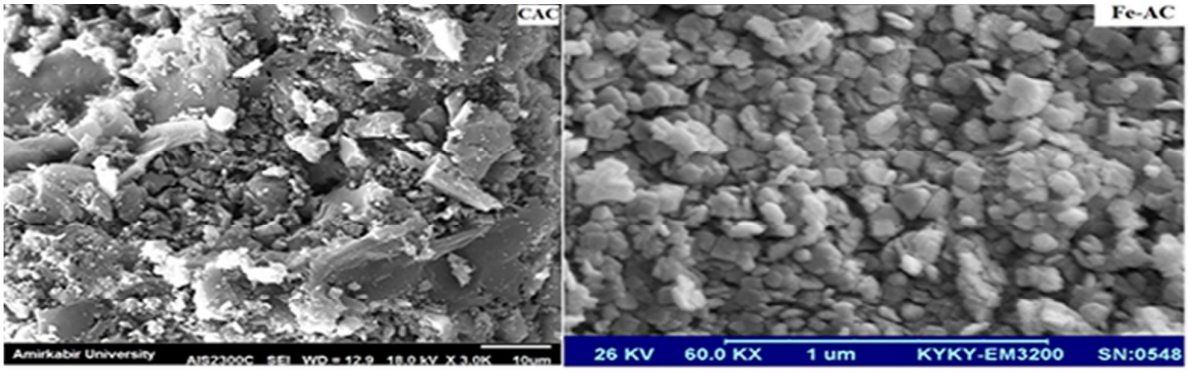

Fig. 1 SEM micrograph of CAC and Fe-AC nanocomposite.

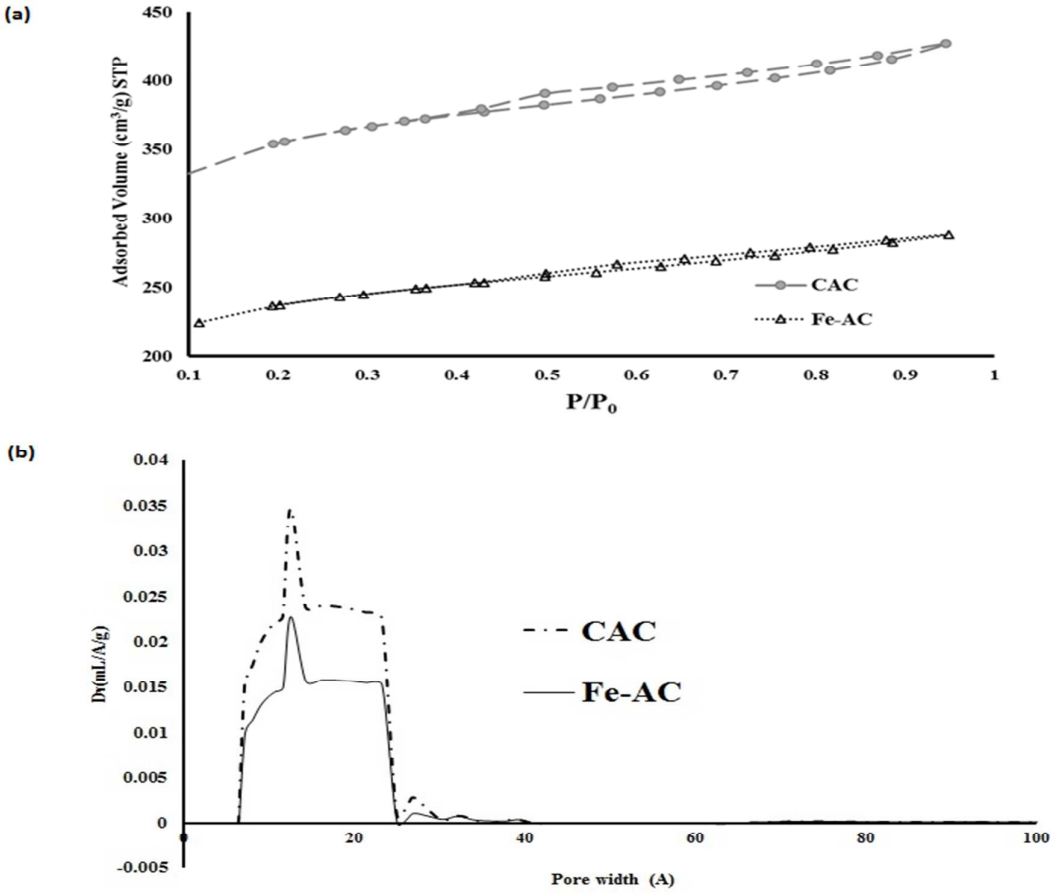

Fig. 2 (a) Adsorption−desorption isotherms of N_2 for CAC and Fe-AC, (b) DFT pore size distribution for CAC and Fe-AC samples.

.

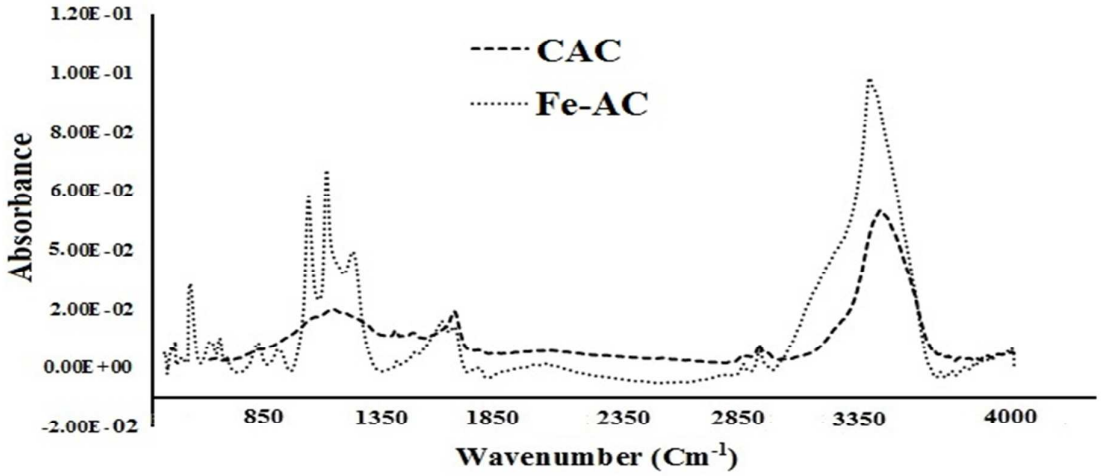

Fig. 3 The FTIR spectra CAC and Fe-AC nanocomposites

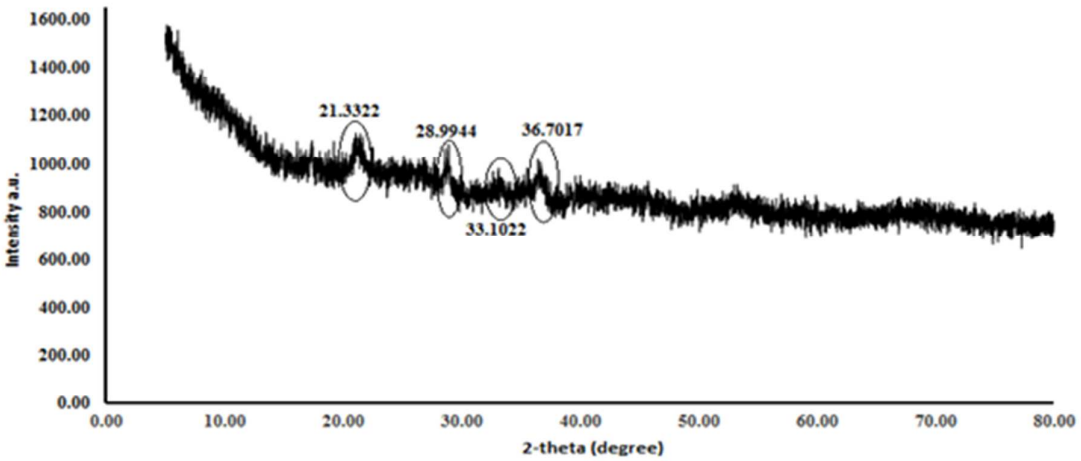

Fig. 4 XRD patternsof Fe-AC nanocomposite**.**

Vanadium ions adsorption

Effect of pH

The results for the effect of the initial pH on vanadium ion adsorption are presented in Fig. 5. The results show that the optimum pH was 4.7 and 4 for CAC and Fe-AC respectively. At pH < pH_{ZPC}, the surface charge of the adsorbent is net positive and this can uptake anions by the electrostatic attraction mechanism [31]. This is due to the fact that the dominant forms of vanadium at initial pH < 3 are cations, and between a pH of 4.0 and 11.0 the anionic forms become dominant [42,43]. The metal adsorption is lowfor pH < 3 due to the repulsion between vanadium cations and the positive surface of adsorbents. By increasing pH (4<pH <5), the anion species of vanadium can be adsorbed by electrostatic attraction. Since the adsorbent surface has a negative charge at higher pH (pH > 5), vanadium adsorption will decrease.

Kinetics and mechanism of adsorption

The relationship between contact time and vanadium ions adsorption using CAC and Fe-AC is illustrated in Fig. 6. As can be seen, the adsorption rate was fast for the first 15 minutes when the adsorption percentage of vanadium reached 50% and 75%, with CAC and Fe-AC respectively. The adsorption process reached the equilibrium at 150 min for CAC and 200 min for Fe-AC.

Generally, the adsorption process involves two types of mechanisms: reaction and mass transfer. The reaction mechanism can be physical or chemical. The mass transfer mechanism has two steps:

1. Film mass transfer or external diffusion: this involves the movement of adsorbate molecules from the bulk of the solution towards the external surface of the adsorbent.

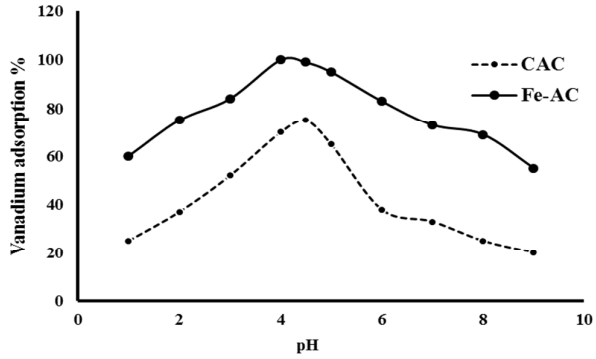

Fig.5 Effect of pH on vanadium adsorption resultsusing CAC and Fe-AC

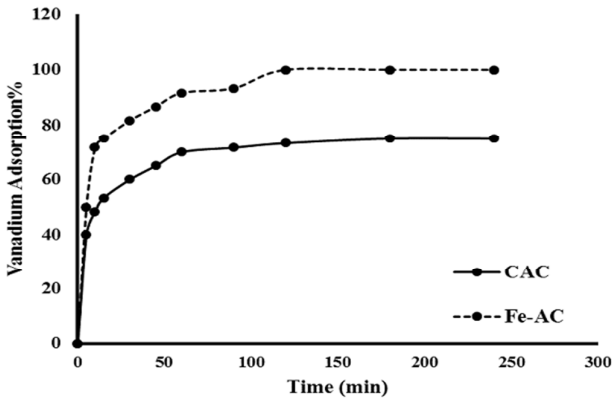

Fig. 6 Effect of time (min) on vanadium adsorption using CAC and Fe-AC.

2. Internalmass transfer or porous diffusion: the adsorbate molecules move into the interior of the adsorbent particles.

It is necessary to determine the slowest (rate controlling) step for the design of the adsorption process. For this purpose, the kinetics data was tested based on pseudo-first-order, pseudo-second-order, intra particle diffusion and Boyd kinetic models. The constants and regression coefficients (R^2) of these models are listed in Table 3. The R^2 values indicate that the pseudo-second order model is more valid than pseudo-first-order model for both adsorbents. Also, the calculated q_e from the pseudo-second-order model is very closely similar to the experimental q_e for vanadium ion adsorption by CAC and Fe-AC. These results confirm the validity of this model for vanadium ion adsorption kinetics, and this suggests that vanadium ion adsorption on CAC and Fe-AC has been controlled by chemical sorption (electrostatic attraction).

According to data presented in Table 3, the R^2 values for the intraparticle model are 0.81 and 0.77 for CAC and Fe-AC respectively. Additionally, the plots do not pass through the origin and have the intercepts (18.6 and 25.78 for CAC and Fe-AC, respectively). Therefore, the intraparticle diffusion is not the rate controlling step.

The Boyd model is applied to distinguish between film diffusion and intraparticle diffusion. The plot of $[-0.4977-\ln(1-F)]$ against time, *t,* can be employed to test the linearity of the experimental values. If the plots are linear and pass through the origin, the rate controlling step in the adsorption process is the internal diffusion. However, if the plots are nonlinear or linear but do not pass though the origin, this process may be controlled by film diffusion. For vanadium ion adsorption on CAC and Fe-AC, the Boyd model has a high R^2 value (98%), but the plots do not pass through the origin and have the interception (0.31 for CAC, 0.449 for Fe-AC). Based on these results, the film diffusion may be important in vanadium ion adsorption by CAC and Fe-AC.

Therefore, both chemical adsorption and film diffusion are involved in the vanadium ion adsorption process. The D_i ($m^2\ s^{-1}$) values were determined to be $1.94e^{-11}$ $m^2\ s^{-1}$ and $5.34e^{-12}$ $m^2\ s^{-1}$ for CAC and Fe-AC respectively. The formation of ferric oxide-hydr(oxide) nanoparticles on the surface of CAC could cause a decrease of the effective diffusion coefficient of solute in the adsorbent phase.

The k_2 value for vanadium adsorption by CAC is higher than adsorption by Fe-AC and this indicates that vanadium adsorption is faster for CAC than Fe-AC.

Longer equilibrium time of Fe-AC nanocomposite compared to the CAC can be explained that the formation of ferric oxide-hydr(oxide)s onto CAC surface is reduced the specified surface area of CAC (according to Table 2). It is expected that the adsorbent with higher surface area and more developed porosity-CAC in the work-has a higher sorption rate than Fe-AC sorbent.

In order to better understand the mechanisms of adsorption, it is necessary to determine the mass transfer resistance. The mas transfer resistance is dependent on either the film (external) diffusion or porous (internal) diffusion, or on both of them. We used a mass transfer model developed by Fulazzaky[42,43] to describe the mass transfer resistance. The mass transfer parameters such as global mass transfer factor $[k_La]_g$, film mass transfer factor $[k_La]_f$ and internal diffusion factor $[k_La]_d$ were determined by mass transfer resistance analysis. The experimental data was analyzed according to following equation:

$$q = B + \frac{1}{\beta} \times \ln(t) \quad (9)$$

where B is potential mass transfer index relating to the driving force of mass transfer (mg g^{-1}) and β is adsorbate–adsorbent affinity parameter (g min mg^{-1}). These parameters are determined from the intercept and slope of plotting q versus ln(t). The R^2 values were 0.975 and 0.979 for CAC and Fe-AC, respectively. The B and β values were determined to be 11.6890 mg g^{-1} and 0.2462 g min mg^{-1} for CAC and 16.8220 mg g^{-1} and 0.1932 g min mg^{-1} for Fe-AC, respectively. Results show that the B value for Fe-AC is higher than for CAC.

The $[k_La]_g(min^{-1})$ is determined using Eq. (10) in accordance with the ratio of C_0/C_f):

$$B = \frac{\ln([k_La]_g) - \ln\left\{\ln\frac{C_0}{C_f}\right\}}{\beta} \quad (10)$$

The $[k_La]_f$ and $[k_La]_d$ (min^{-1}) is calculated according to the following equations:

$$[k_La]_f = [k_La]_g \times e^{-\beta q} \quad (11)$$

$$[k_La]_d = [k_La]_g - [k_La]_f \quad (12)$$

Fig. 7 shows the variation of $[k_La]_g$, $[k_La]_f$and $[k_La]_d$ versus C_f/C_0. This figure reveals that the variation of these mass transfer factors for vanadium adsorption onto Fe-AC is higher than for CAC. Because formation of ferric nanoparticles on surface of CAC creates new functional groups (or more positive adsorption sites) and chemisorption is more important for vanadium adsorption onto Fe-AC [42]. As can be seen, the curves for these mass transfer factors are comparable. It can be concludethat resistance of mass transfer is dependent on both the external diffusion and internal diffusion for both adsorbents.

Adsorption Equilibrium

The effect of initial concentration of vanadium on the adsorption process was studied to identify the equilibrium conditions and maximum sorption capacity of adsorbents. This can be described and accomplished by using the various well-known adsorption isotherm models. Fig. 8 shows the adsorption isotherms of vanadium on CAC and Fe-AC at various temperatures. The sorption equilibrium data was fitted for the linear Langmuir, Freundlich and D-R isotherms. Constant parameters and regression coefficient (R^2)

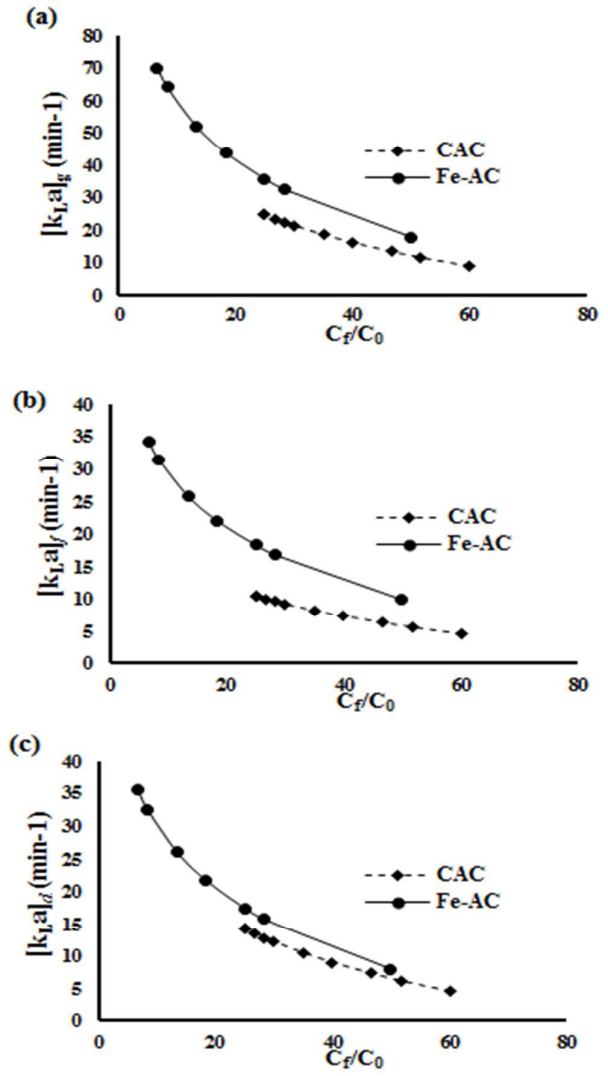

Fig. 7 Variation of Mass transfer factors: a: $[k_La]_g$, b: $[k_La]_f$, c: $[k_La]_d$.

Table 3 Constants and regression coefficients for kinetic models

Parameters		CAC	Fe-AC
$q_{e,exp}$		32.140	42.857
Pseudo-first order	k_1	0.020	0.022
	q_e	14.240	16.622
	R^2	0.960	0.910
Pseudo second-order	k_2	0.004	0.005
	q_e	32.890	42.016
	R^2	1.000	1.000
Boyd model	B	0.026	0.022
	Intercept	0.310	0.449
	R^2	0.980	0.980
Intraparticle diffusion	k_{id}	1.070	1.350
	Intercept	18.600	25.780
	R^2	0.810	0.770

for these isotherms are reported in Table 4. Based on D-R isotherm parameters, the mean free energy E (kJ mol^{-1}) of adsorption per molecule of the adsorbate was 11.1 kJ mol^{-1} for CAC and 12.9 kJ mol^{-1} for Fe-AC.

These values correspond to the ion-exchange process and electrostatic attraction (chemical sorption).

According to Table 4, the Freundlich model provided the best-fitted isotherm for the equilibrium data of vanadium ion adsorption by CAC and Fe-AC at all temperatures. This may be attributed to the coexistence of different sorption sites and/or different sorption mechanisms or the sorption of different vanadium species that have led to a heterogeneous adsorption. As it can be seen in Table 4, the maximum adsorption capacity of Fe-AC is higher than CAC (about 215%). This higher capacity may be related to the availability and particle size of the ferric nanoparticles loaded onto CAC. These nanoparticles create new positive adsorption sites for vanadium anions on the CAC surface. The maximum vanadium ion adsorption capacity for other adsorbents is listed in Table 5 for a better comparison [28, 34, 44-51]. Thiscomparison indicates that CAC and Fe-AC adsorbents exhibit a reasonable capacity for vanadium adsorption from aqueous solutions.

Thermodynamic parameters

According to Fig. 8, it is clear that the adsorption capacity decreases as temperature increases. These equilibrium data was fitted for the linear Langmuir model and the values of K_L were used to determine the thermodynamic parameters according to the following equations:

$$\Delta G^\circ = -RT\ln(K_L) \quad (13)$$

$$\ln(K_L) = \frac{-\Delta H^\circ}{RT} + \frac{\Delta S^\circ}{R} \quad (14)$$

$$T.\Delta S^\circ = \Delta H^\circ - \Delta G^\circ \quad (15)$$

where ΔG° (kJ mol^{-1}), ΔH°(kJ mol^{-1}) and ΔS°(kJ mol^{-1}) are the changes in free energy, enthalpy, and entropy respectively. R is the universal gas constant (8.314 J mol^{-1} K^{-1}) and T (°K) is temperature. ΔH° and ΔS° can be obtained from the slope and intercept of plotting ln (K_L) versus 1/T (Fig. 9). These thermodynamic parameters are presented in Table 6. The negative values of ΔG°, ΔH° and ΔS° indicate that vanadium ion adsorption by CAC and Fe-AC has a spontaneous, exothermic nature and is feasible.

Reuse results

The results for adsorption-desorption cycles of vanadium are presented in Fig. 10. As the results show, the adsorption percentage of vanadium decreased from 75.5 % to 45.1% for CAC and 99.8% to

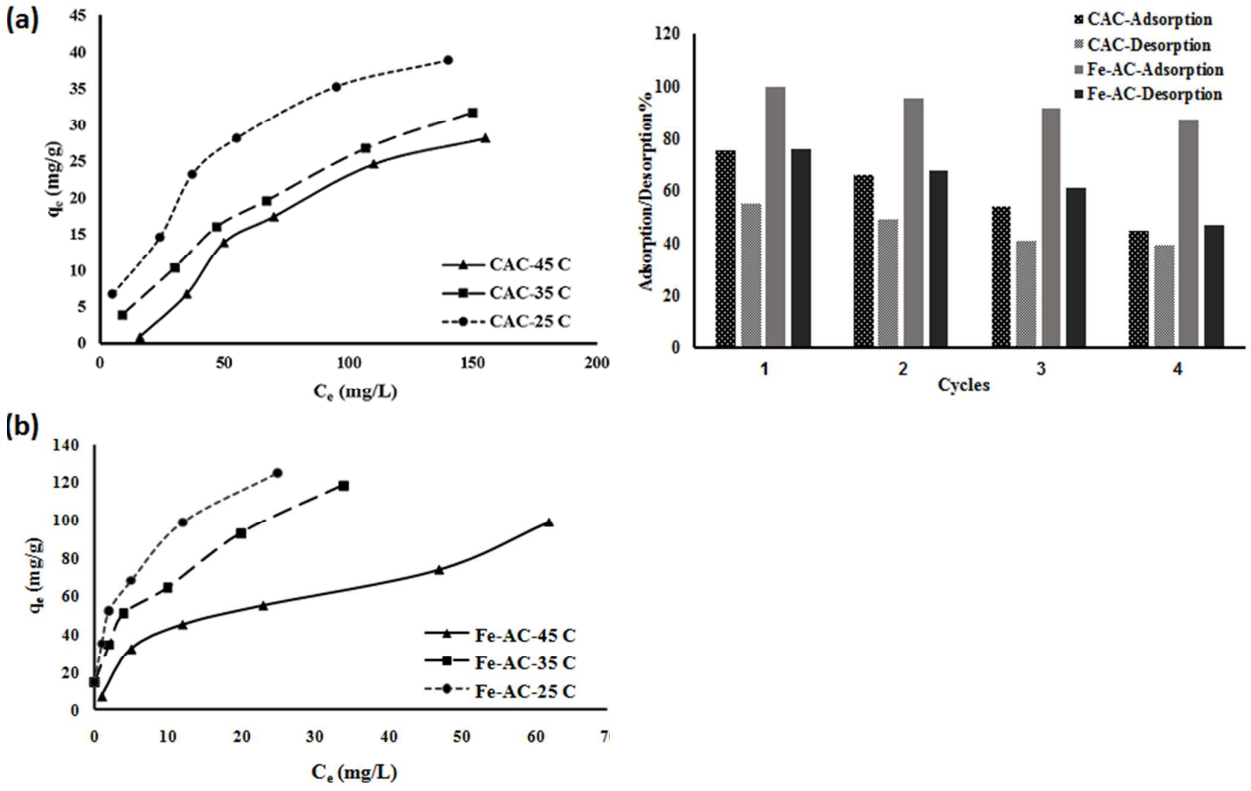

Fig. 8 Equilibrium isotherms of vanadium adsorption at different temperatures using: (a) CAC, (b) Fe-AC nanocomposites.

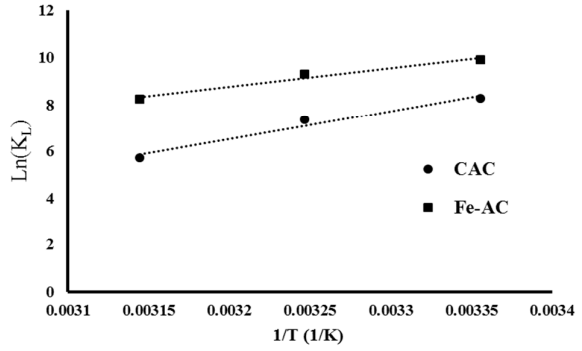

Fig. 9 Relationship between ln (K_L) and 1/T for vanadium adsorption

87.5% for Fe-AC, respectively, after four cycles. The results indicated that the adsorption ability of the Fe-AC for vanadium could still be maintained at over 85% level in the fourth adsorption/desorption cycle.

Therefore its potential for vanadium adsorption has been remain high in these cycles yet. . The 0.10HCl solution was chosen because our preliminary desorption tests showed that this solution was the best extractant for vanadium desorption between H_2SO4, NaOH and Na_2CO_3 solutions for two adsorbents. Results showed that the repulsion between vanadium cations and the positive surface of the adsorbent in the acidic solution (pH < 2-3) causes to vanadium desorption from the adsorbent surface. As regards vanadium cations belong to the hard acids group according to Pearson theory[52], it is expected that HCl performs better than H_2SO_4 for vanadium extraction from the saturated sorbents. This is due to the easier and stronger interaction of vanadium cations with the borderline base Cl^{1-} compared to their interaction with SO_4^{2} (Cl^{1-} is harder base than SO_4^{2}).

Fig. 10 Adsorption\desorption cycles for vanadium adsorption with CAC and Fe-AC.

Table 6 Thermodynamic parameters for vanadium ions adsorption

Adsorbent	Temp. (K)	ΔG° kJ mol^{-1}	ΔH° kJ mol^{-1}	$T.\Delta S^{\circ}$ kJ mol^{-1}	ΔS° kJ mol^{-1}	R^2
CAC	298	-20.47	-100.18	-79.27	-0.26	0.97
	308	-18.84		-81.93		
	318	-15.11		-84.59		
Fe-AC	298	-24.56	-65.57	-40.53	-0.13	0.97
	308	-23.84		-41.88		
	318	-21.79		-43.25		

Conclusion

In this work, a composite of activated carbon and ferric oxide-hydr(oxide) nanoparticles (Fe-AC) has been synthesized as a new adsorbent in order to an improvement of vanadium removal. The adsorptive performance of CAC and Fe-AC for vanadium was investigated under various conditions. The results indicate that Fe-AC has an effective vanadium ion adsorptive capability.The adsorption efficiency was affected by pH of the solution, and the maximum vanadium ion adsorption was found at a pH of 4.7 and 4 for CAC and Fe- AC respectively. At optimum pH, CAC and Fe-AC could adsorb 74% and 100% of vanadium after 3 h. The kinetic results showed that chemical adsorption and film diffusion were important steps in vanadium ion adsorption using CAC and Fe-AC. The Freundlich model was the best model to describe equilibrium adsorption of vanadium ions with these adsorbents. The Fe-AC nanocomposite has a higher capacity for vanadium ion adsorption (119.01 mg g^{-1}) than CAC (37.87 mg g^{-1}).

Acknowledgements

The authors acknowledge with a great degree of appreciation, that this project was financially supported by a research grant (research project No.:61736) from Iran Nano Technology Initiative Council, in Iran. The authors sincerely thank Mrs. Tahereh Doostmohammadi for analyzing the samples by AAS.

Table 4 Constants parameters and regression coefficients for Langmuir, Freundlich and R-D isotherms. (C_0=20-200 mg L^{-1}, m=1g L^{-1}, V=50 mL).

Isotherm	Parameter	25 °C		35 °C		45 °C	
		CAC	Fe-AC	CAC	Fe-AC	CAC	Fe-AC
Langmuir	K_L (L mg^{-1})	0.076	0.397	0.038	0.217	0.005	0.074
	q_{max} (mg g^{-1})	37.780	119.010	34.300	111.900	27.810	103.100
	R^2	0.940	0.970	0.960	0.960	0.950	0.950
Freundlich	K_f	5.220	37.020	2.320	26.214	0.215	9.036
	n	2.280	2.600	1.820	2.370	0.950	1.703
	R^2	0.990	0.990	0.980	0.980	0.980	0.980
D-R	β (mol^2 J^{-2})	4e-9	3e-9	6e-9	4e-9	1e-8	6e-9
	q_m (mol g^{-1})	0.003	0.008	0.002	0.007	0.002	0.007
	R^2	0.960	0.960	0.960	0.960	0.095	0.970

Table 5 Adsorption capacity of different adsorbents for vanadium ions adsorption.

Adsorbent	Adsorption capacity (mg g^{-1})	Initial pH	Adsorbent dose (g L^{-1})	Initial concentration (mg L^{-1})	Ref.
Protonated chitosan flakes (PCF)	12.22	4.4-5.0	5.0	1-5	28
$ZnCl_2$-modifed activated carbon	24.90	4.0-9.0	4.0	40-120	34
Calcined Mg/Al hydrotalcite	513.00	3.0	0.2	10-50	44
PGTFS–$NH_3^+Cl^-$	45.86	6.0	2.0	10-300	45
Crosslinked chitosan	6.27	4.0-4.5	0.6	-	46
metal sludge	24.80	7.6	10.0	10-50	47
Zr(IV)-impregnated collagen fiber	137.96	5.0	1.0	100-600	48
Fe(III)/Cr(III)hydroxide waste	11.43	4.0	10.0	10-40	49
His-MWCNTs	4.85	5.5	0.8	1-8	50
Zr(IV)-loaded orange juice residue	51.90	2.5	2.0	-	51
CAC	37.78	4.5	1.0	25.0-200.0	This work
Fe-AC	119.01	4.5	1.0	25.0-200.0	This work

Notation

k_1	Pseudo-first-order rate constant (min^{-1})
k_2	Pseudo-second-order rate constant (g mg^{-1} min^{-1})
k_{id}	Intra-particle diffusion rate constant (mg g^{-1} $min^{-1/2}$)
D_i	Effective diffusion coefficient (m^2 s^{-1})
q	Amount of solute adsorbed per unit weight of adsorbent (mg g^{-1}) at t
q_e	Amount of solute adsorbed per unit weight of adsorbent (mg g^{-1}) at equilibrium
r	Radius of the adsorbent particles (m)

References

[1] M. P. Deosarkar, S. M. Pawar and B. A. Bhanvase, *Chem. Eng. Process*., 2014, **83**, 49-55.

[2] L. M. Pastrana-Martíneza, N. Pereirab, R. Limab, J. L. Fariaa, H. T. Gomesa and A. M. T. Silva, *Chem. Eng. J*., 2015, **261**, 45–52.

[3] X. Cui, S. Belo, D. Krüger, Y. Yan, R. T. De Rosales, M. Jauregui-Osoro,H. Ye and et al., Biomaterials, 2014, **35**, 5840–5846.

[4] Y. Zhang, J. Shen, H. Yang, Y. Yang, Z. Zhou and Z.A. Yang, *Sensor. Actuat. B-Chem*., 2015, **207**, 887-892.

[5] T. J. Tu, C. F. You, C. K. Chang and M. H. Chen, *J. Taiwan Inst. Chem. E*., 2015, **46**, 148-154.
[6] A. Uheida, M. Iglesias, M. Fontàs, M. Hidalgo, V. Salvadó, Y. Zhang and M. Muhammed, *J. Colloid. Interf. Sci*., 2006, **301**, 402–408.
[7] Z. Zhang and J. Kong, *J. Hazard. Mater*., 2011, **193**, 325-329.
[8] Z. Lou, Z. Zhou, W. Zhang, X. Zhang, X. Hu, P. Liu and H. Zhang, *J. Taiwan Inst. Chem. E*., doi:10.1016/j.jtice.2014.11.007.
[9] K. Kalantari, M. Ahmad, H. R. Fard-Masoumi, K. Shameli, M. Basri and R. Khandanlou, *J. Taiwan Inst. Chem. E*.,doi: 10.1016/ j.jtice.2014.10.025.
[10] M. Ghaedi, S. Hajjati, Z. Mahmudi, I. Tyagi, S. Agarwal, A. Maity and V.K. Gupta,*Chem. Ing. J*., 2015, **268**, 28-37.
[11] A. Mohammadi, H. Daemi and M. Barikani, *Int. J. Biol. Macromol*., 2014, **69**, 447-455.
[12] Y. Chen and S. Mu, *Sensor. Actuat. B-Chem*., 2014, **192**, 275–282.
[13] M. Kavand, T. Kaghazchi and M. Soleimani, *Korean J. Chem. Eng*., 2014, **31**, 692-700.
[14] R. Asadi-Kesheh, S. A. Mohtashami, T. Kaghazchi, N. Asasian and M. Soleimani, *Sep. Sci. Technol*., 2015, **50**, 223–232.
[15] H. Sharififard, F. Zokaee and M. Soleimani, *Asia-Pacific J. Chem. E*., 2013, **8**, 384-95.
[16] M. Barkat, D. Nibou, S. Chegrouche and A. Mellah,*Chem. Eng. Process*., 2009, **48**, 38-47.
[17] N. Asasian, T. Kaghazchi and M. Soleimani, *J. Ind. Eng. Chem*., 2012, **18**, 283–289.
[18] J. H. Xu, N. Gao, Y. Deng and S. Xia, *Chem. Ing. J*., 2013, **222**, 520-526.
[19] A. M. Cooper, K. D. Hristovski, T. M◌̈ller, P. Westerhoff and P. Sylvester, *J. Hazard. Mater*., 2010, **183**, 381–388.
[20]N. Mehrabi, M. Soleimani, M. MadadiYeganeh and H. Sharififard, RSC Adv., 2015, **5**, 51470.
[21] T. Depci,*Chem. Eng. J*., 2012, **181-182**, 467-478.
[22] H. Zhu, Y. Jia, X. Wu and H. Wang, *J. Hazard. Mater*., 2009, **172 (2-3)**, 1591-1596.
[23] B. Kakavandi, R. RezaieKalantary, A. JonidiJafari, S.Nasseri, A. Ameri, A. Esrafili and A. Azari, *CLEAN–Soil Air Water*,doi: 10.1002/clen.201200568.
[24] E. Deliyanni, T.J. Bandosz, *J. Hazard. Mater*., 2011, **186(1)**, 667-674.
[25] C. S. Castro, M. C. Guerreiro, L. C. A. Oliveira, M. Gonc¸alves, A. S. Anasta´ cio and M. Nazzarro, *Appl. Catal. A: Gen*., 2009, **367 (1-2)**, 53-58.
[26] H. Wyers,*Brit. J. Ind. Med*., 1946, **3**, 177–182.
[27] B. Patel, G.E. Henderson, S. J. Haswell and R. Grzeskowiak, Analyst.,1990, **115**, 1063–1066.
[28] A. Padilla Rodríguez, J.A. Hernández Viezcas, J.R. Peralta Videa, G.L. GardeaTorresdey, O. Perales Pérez and F. R. Román Velázquez, *Microchem. J*., 2015, **118**, 1–11.
[29] A. Alibrahim, H. Shlewit and S. Alike, *Chem. Eng. J*., 2008, **52/1**, 29–33.
[30] M. Nabavinia, M. Soleimani and A. Kargari, *Int. J. Chem. Environ. Eng*.,2012, **3**, 149-152.
[31] H. Sharififard, M. Soleimani and F. Zokaee Ashtiani,*J. Taiwan Inst. Chem. E*., 2012, **43 (5)**, 696–703.
[32] S. Lowell, J. E. Shields, M. A. Thomas and M. Thommes, *Characterization of Porous Materials and Powders: Surface Area, Pore Size and Density*, Springer, Dordrecht, 2004.
[33] F. B. Aarden, *Adsorption onto Heterogeneous Porous Materials: Equilibria and Kinetics*, Ph.D. Dissertation, TechnischeUniversiteit, Eindhoven, Eindhoven, 2001.
[34] C. Namasivayam and D. Sangeetha, Adsorption, 2006, **12**, 103–117.
[35] S. J. Gregg and K. S. Sing, *Adsorption, Surface Area, and Porosity,* Academic Press, New York, 1982.
[36] K. S. W. Sing, *Pure. Appl. Chem*., 1985, **57**, 603-619.
[37] J. H. Chua, *The Adsorption of Fatty Acids Using Metal Silica Complexes from Rice Husk Ash*, Master's Dissertation, Penang, UniversitiSains Malaysia, 2008.
[38] Z. Al-Qodah and R. Shawabkah, *Braz. J. Chem. Eng*., 2009, **26**, 127–136.
[39] S. Hydari, H. Sharififard, M. Nabavinia and M. R. Parvizi, *Chem. Eng. J*., 2012, **193–194**, 276–282.
[40] Y. Li, C. Zhu, T. Lu, Z. Guo, D. Zhang, J. Ma and S. Zhu, *Carbon*, 2013, **52**, 565 –573.
[41] P. Cambier, *Clay Miner*., 1986, **21**, 191-200.
[42]M. A. Fulazzaky, *Chem. Eng. J*.,2011,**166**, 832–840.
[43]M. A. Fulazzaky, M.H.Khamidun, R. Omar, *Chem. Eng. J*.,2013, **228**, 1023–1029.
[44] T. Wang, Z. Cheng, B. Wang and W. Ma, *Chem. Eng. J*., 2012, **181-182**, 182-188.
[45] T. S. Anirudhan and P. G. Radhakrishnan, *Chem. Eng. J*., 2010, **165**, 142–150.
[46] S. Qian, H. Wang, G. Huang, S. Mo and W. Wei, *J. Appl. Polym. Sci*., 2004, **92**, 1584–1588.
[47] A. Bhatnagar, A. Kumar Minocha, D. Pudasainee, H. K. Chung, S. H. Kim, H. S. Kim, G. Lee and at el., *Chem. Eng. J*., 2008, **144**, 197–204.
[48] X. Pin Liao, W. Tang, R. Qing Zhou and B. Shi, *Adsorption*, 2008, **14**, 55–64.
[49] K. Prathap and C. Namasivayam,*Environ. Chem. Lett*., 2010, **8**, 363–371.
[50] Y. Liu, Y. Li and L. Yang, *Microchem. J*., 2012, **104**, 56–61.
[51] Q. Hu, H. Paudyal, J. Zhao, F. Huo, K. Inoue and H. Liu, *Chem. Eng. J*., 2014, **248**, 79-88.
[52] R.G. Pearson, *Inorg. Chem*.,1988, **27**, 734–740.